Polish Society of Composite Materials
Polskie Towarzystwo Materiałów Kompozytowych

14: 3 (2014) 169-173

COMPOSITES THEORY AND PRACTICE

Anna Marzec[1]*, Anna Kusior[2], Marta Radecka[2], Zbigniew Pędzich[1]

[1] AGH - University of Science and Technology, Faculty of Materials Science and Ceramics, Department of Ceramics and Refractory Materials, al. Mickiewicza 30, 30-059 Krakow, Poland
[2] AGH - University of Science and Technology, Faculty of Materials Science and Ceramics Department of Inorganic Chemistry, al. Mickiewicza 30, 30-059 Krakow, Poland
**Corresponding author. E-mail: amarzec@agh.edu.pl*

Received (Otrzymano) 26.08.2014

PREPARATION OF NANOCRYSTALLINE COMPOSITES TiO_2-SnO_2 BY SOL-GEL METHOD

The paper describes the sol-gel method for preparing nanocomposites from the TiO_2-SnO_2 system with various chemical compositions. The obtained nanopowders are characterized by a significantly expanded specific surface area (SSA ~ 100 m^2/g), which suggests low particles agglomeration and undoubtedly has a beneficial effect on the application of the obtained nanopowders in the production of resistive sensors for gas detection. The crystallites sizes estimated with use of XRD (D_{hkl} ~ 8 nm) are similar to those calculated based on specific surface area measurements (D_{BET} ~ 15 nm). Moreover, the paper examines the spectral dependence of the diffuse reflection coefficient $R_{diff}(\lambda)$ of the obtained nanocomposites.

Keywords: nanopowders, TiO_2-SnO_2 nanocomposites, resistive gas sensors

OTRZYMYWANIE NANOKRYSTALICZNYCH KOMPOZYTÓW TiO_2-SnO_2 METODĄ ZOL-ŻEL

W pracy opisano metodę zol-żel do otrzymywania nanokompozytów z układu TiO_2-SnO_2 o różnym składzie chemicznym. Otrzymane nanoproszki charakteryzują się dużym rozwinięciem powierzchni właściwej (SSA ~100 m^2/g), co sugeruje słabą aglomerację cząstek i niewątpliwie wpływa korzystnie na zastosowanie otrzymanych nanoproszków do wytwarzania sensorów rezystancyjnych dla wykrywania gazów. Wielkości krystalitów wyznaczone techniką XRD (D_{hkl} ~ 8 nm) są zbliżone do oszacowanych na podstawie pomiarów powierzchni właściwych (D_{BET} ~ 15 nm). W pracy zbadano również spektralną zależność współczynnika odbicia dyfuzyjnego $R_{diff}(\lambda)$ uzyskanych nanokompozytów.

Słowa kluczowe: nanoproszki, nanokompozyty TiO_2-SnO_2, rezystancyjne sensory gazowe

INTRODUCTION

Resistive sensors belong to a group of sensors in which gas, as a result of its adsorption on the sensor surface, alters electrical properties. In the presence of an oxidizing gas (NO_x) in the examined atmosphere, the resistance of the sensor material, which is an n-type semiconductor, rises, whereas in the presence of reductive gases (H_2, CH_4) it falls. The detection mechanism may be more complex when there are two opposing processes taking place, e.g., in the case of ammonia detection (a decrease in resistance due to the presence of ammonia and rise due to the formation of NO_x) [1, 2].

Metal-oxide-based chemical sensors, which have been used over an extensive period of time, are characterized by high sensitivity, however, their key disadvantage is limited selectivity. The interest in metal-oxide-based nanocomposite materials (e.g. SnO_2-ZnO, Fe_2O_3-ZnO, Fe_2O_3-SnO_2, WO_3-SnO_2, TiO_2-SnO_2) has risen in recent years [3, 4]. The use of such systems allows one to improve sensor parameters such as selectivity and sensitivity, as well as to decrease the operating temperature.

Tin (IV) oxide SnO_2 is called a surface sensor due to its small electron depletion area during adsorption in contrast to TiO_2, which is characterized by a volume mechanism of interaction with the gas phase. SnO_2 is characterized by high sensitivity at the temperature ranging from 300÷400°C and process reversibility. The main disadvantages of this material are lack of selectivity and low thermodynamic stability at high temperatures and in reductive atmospheres, while the main advantages of titanium dioxide are the wide range of oxygen partial pressure from 10^{-18} to 10^5 Pa and the ability to function at high temperatures ranging from 700 to 1200°C. It is limited by the high resistance of TiO_2, possible occurrence of anatase/rutile phase transition and a conductivity-type change from n to p. The basic objective in applying nanocomposites as junctions

in the said oxides is modification of the electron configuration resulting from interaction between both components. Direct contact between the grains causes band curvature and the observed charge transfer from TiO_2 to SnO_2 is caused by an electronic band location difference and conductivity difference [4, 6].

Nanocrystalline metal oxides are obtained by various methods. One of the most commonly applied methods is the hydrothermal method, nevertheless, also the sol-gel method and reaction in the solid phase are used. These methods allow one to obtain nanostructures of various forms, which find applications not only in sensor technology, but also in nanoelectronics, optoelectronics and heterogeneous photocatalysis [7-9].

In this paper, the synthesis of TiO_2-SnO_2 nanocrystalline composites using the sol-gel method has been presented, as well as the correlation between the structure and chemical composition and selected physicochemical properties of TiO_2-SnO_2 composites have been presented.

MATERIALS AND METHODS

Sample preparation

Nanocomposites were obtained by means of the two-stage sol-gel method in which the metal-organic titanium(IV) oxide compound and hydrated tin(IV) chloride were used as the original compounds. At the first stage of the synthesis, nanocrystalline TiO_2 was obtained, which then was used to prepare a nanocomposite powder. TiO_2 was obtained by hydrolysis of the metal-organic original compound - titanium isopropoxide (Avantor 98% p.a. grade) ten times diluted in anhydrous isopropyl alcohol (Avantor 98% p.a. grade). Since the solution pH affects the size of the obtained crystallites, HCl (Avantor 36% p.a. grade) and CH_3COOH (Avantor 27% p.a. grade) were added to the alcohol at a ratio of 1:10 by volume to adjust the pH to 3. Next, the solution was mixed for 30 minutes at room temperature and then added drop by drop to H_2O and stirred intensively at the same time. The stirring was continued for an hour at room temperature. The $Ti[(OCH(CH_3)_2)]_4$:H_2O ratio in the prepared solution was 1:8 by volume. After hydrolysis, the particle condensation and sol formation stage occurred. The sol was changed into gel with a structure containing an occluded solvent. The solvent was removed from the gel by evaporation by drying at 115°C for 18 hours. In order to obtain a crystalline phase and to remove the remains of organic substances, the system was subjected to calcination at 400°C for 2 hours. The calcination temperature was estimated based on the performed TG/DSC analysis (Netzsch STA 409). The sample was heated in air atmosphere at a heating speed of 10°C/min to the target temperature of 800°C. The results of the analysis are presented in Figure 1. On the TG curve, two distinct weight loss intervals of different size may be specified. The first (loss in weight: 13.41%) up to approx. 250°C is related to the loss of excessive amounts of water and the occluded solvent. On the DSC curve, weak endothermic peaks are visible within the discussed range of temperature. The second stage of weight loss (7.08%) occurs at temperatures ranging from 250 to 400°C. The exothermic peaks of 257.9 and 342.5°C on the DCS curve related to heat generation result from the combustion of organic compound degradation products used for producing TiO_2. Another change in enthalpy on the DSC curve may be related to the phase transition of TiO_2 anatase into rutile at the extreme temperature of 593.4°C. The reactions occurring during TiO_2 synthesis are:

1. $Ti[(OCH(CH_3)_2]_4 + 4H_2O \rightarrow Ti(OH)_4 + 4(CH_3)_2CHOH$ (25°C) (1)

2. $Ti(OH)_4 \rightarrow TiO_2$ (amorphous) $+ 2H_2O$ (115°C) (2)

3. $(CH_3)_2CHOH + 9/2O_2 \rightarrow 3CO_2 + 4H_2O$ (250÷350°C) (3)

4. $CH_3COOH + 2O_2 \rightarrow 2CO_2 + 2H_2O$ (250÷350°C) (4)

5. TiO_2 (amorphous) $\rightarrow TiO_2$ (crystalline) (400°C) (5)

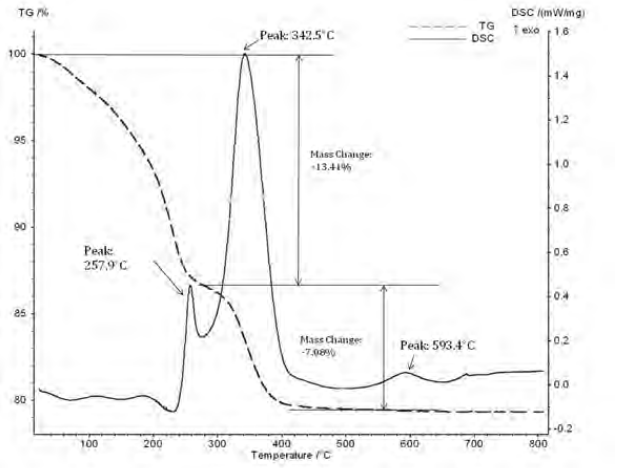

Fig. 1. TG/DSC analysis of initial gel for obtaining TiO_2

Rys. 1. Analiza TG/DSC żelu wyjściowego dla otrzymania TiO_2

The second stage of nanocomposite synthesis was to introduce SnO_2 nanoparticles into the system. The original compound for SnO_2 was $SnCl_4 \cdot 5H_2O$, of which an appropriate amount (as shown in Table 1) was dissolved in isopropyl alcohol (Avantor 98% p.a. grade) in order to obtain a 3.27 mol/dm^3 concentration solution. The prepared solution was stirred for 30 minutes at 30°C. The next steps undertaken were exactly like in the production of TiO_2 (the solution was ten times diluted, pH adjusted to 3, stirred for 30 minutes) and dripped into the colloidal solution prepared by dispersing an adequate amount of TiO_2 (as shown in Table 1) in an adequate amount of water (Fig. 2), so that the

$SnCl_4$ solution in isopropyl alcohol to H_2O ratio was 1:8 by volume. Then, the sol obtained in the above described way was changed into gel, which was then dried at 115°C for 18 hours and calcined at 540°C for 2 hours in the next stage. The calcination temperature was adjusted based on the TG/DSC gel analysis (Fig. 1) so that the TiO_2 anatase/rutile phase transition in the obtained composite nanopowders can be avoided. Thus, a TiO_2-SnO_2 composite was obtained, which was characterized later.

TABLE 1. **Assumed mass fractions of oxides in composite nanopowders**

TABELA 1. **Założone udziały masowe tlenków w nanoproszkach kompozytowych**

Sample no.	Mass fractions [%]
1	SnO_2 - 0%; TiO_2 - 100%
2	SnO_2 - 10%; TiO_2 - 90%
3	SnO_2 - 20%; TiO_2 - 80%
4	SnO_2 - 60%; TiO_2 - 40%

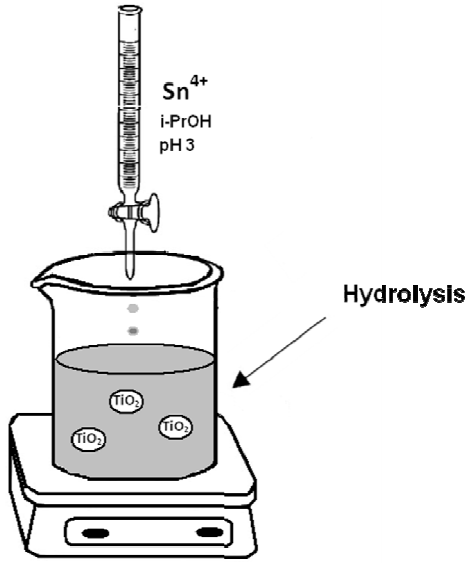

Fig. 1. Synthesis process diagram of TiO_2-SnO_2composite nanopowder

Rys. 1. Schemat procesu syntezy nanoproszku kompozytowego TiO_2-SnO_2

Methods used in characterizing obtained composite nanopowders

In the case of nanocrystalline powders, the most important parameters characterizing the material are its phase composition and grain size.

The former of these two parameters was estimated using an X'Pert Pro X-ray diffractometer produced by the PANalytical company. XRD was also used for specifying the mean crystallite size by means of the Scherrer equation.

The grain size was estimated by direct observation of the powders with a TECNAI FEG transmission electron microscope (TEM) produced by FEI (200 kV).

Additionally, the mean particle sizes were calculated by means of powder specific surface area measurements based on the BET physical adsorption isotherm. The measurements were performed on a NOVA 1200e analyzer by Quantachrome Instruments with nitrogen as the adsorbate. The mean particle sizes of the powders were estimated based on the values of specific surface areas using correlations (6) and (7):

$$D_{BET} = \frac{6000}{d \cdot S_w}[\text{nm}] \tag{6}$$

$$d = d_1 \cdot V_1 + d_2 \cdot V_2 \tag{7}$$

where: d - the actual density of the material [g/cm^3]; d_1 - density of the first component [g/cm^3]; d_2 - density of the second component [g/cm^3]; V_1 - volume fraction of the first component; V_2 - volume fraction of the second component; SSA - specific surface area of the powder measured using the BET physical adsorption isotherm [m^2/g]. The density values for TiO_2 (anatase) and SnO_2 (cassiterite) are estimated at, respectively, 3.8 and 6.9 g/cm^3. The optical parameters of the nanopowders were estimated by spectrophotometric measurements of the light reflectance factor performed by means of a Perkin Elmer LAMBDA 19 double-beam spectrophotometer equipped with an integrating sphere at wavelengths ranging from 250 to 750 nm.

RESULTS AND DISCUSSION

Characteristics of obtained composite nanopowders

In Figure 3, diffractograms of the TiO_2 oxide and its TiO_2-SnO_2 composites are presented. Titanium(IV) oxide crystallizes in an anatase tetragonal structure; the crystallite size calculated based on the width of diffraction peaks (110) is estimated at approx. 8 nm. In the case of other materials, additional SnO_2 cassiterite reflections are observed.

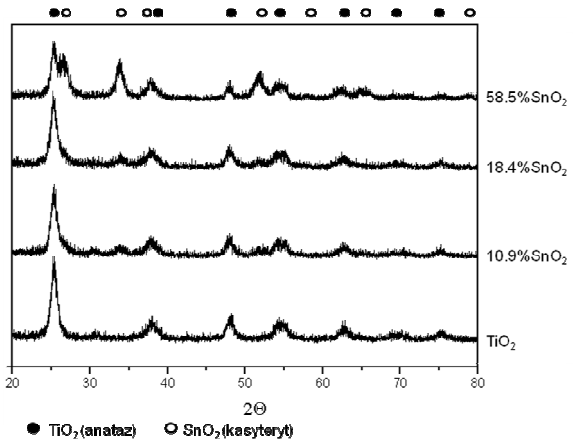

Fig. 3. XRD diffractograms of synthesized nanopowders

Rys. 3. Dyfraktogramy XRD zsyntetyzowanych nanoproszków

For nanocomposites with up to 18.4% weight fraction SnO_2, the strongest (110) SnO_2 peak is not visible. This is caused by an overlap of reflections from (110)

pure oxide TiO_2 ($2\Theta = 25.31^o$) and SnO_2 ($2\Theta = 26.70^o$) surfaces and a rise in the width of diffraction peaks resulting from crystallite sizes ranging from 5 to 10 nm. The mean crystallite size and weight fraction of both phases estimated based on X-ray examinations are presented in Table 2.

TABLE 2. **Oxide mass fractions specified with XRD and powder particle sizes estimated using various methods**
TABELA 2. **Udziały masowe tlenków wyznaczone techniką XRD oraz rozmiary cząstek proszków wyznaczone różnymi metodami**

Sample no.	Mass fractions (XRD) [%]	Average nanoparticle size (XRD) D_{hkl} [nm]	Specific surface area SSA [m^2/g]	Estimated particle size D_{BET} [nm]
1	SnO_2 - 0%; TiO_2 - 100%	TiO_2 - 8.0 ± 0.2	119.83 ±5.2	13.18 ±1.2
2	SnO_2 - 10.9%; TiO_2 - 89.1%	TiO_2 - 8.3 ±0.2 SnO_2 - 4.8 ±0.2	110.02 ±5.2	13.67 ±1.2
3	SnO_2 - 18.4%; TiO_2 - 81.6%	TiO_2 - 7.8 ±0.2 SnO_2 - 5.3 ±0.2	92.57 ±5.2	15.66 ±1.2
4	SnO_2 - 58.5%; TiO_2 - 41.5%	TiO_2 - 10.1 ±0.2 SnO_2 - 5.5 ±0.2	116.05 ±5.2	10.36 ±1.2

The TEM observations of the composite powder containing 10.9% SnO_2 performed at various magnifications are presented in Figure 4. Based on these observations the obtained powder was found to be agglomerated, yet the formed grain agglomerations are relatively loose. In the images, individual grains of the size of several nanometers, similar to the crystallite sizes specified by XRD, may be differentiated.

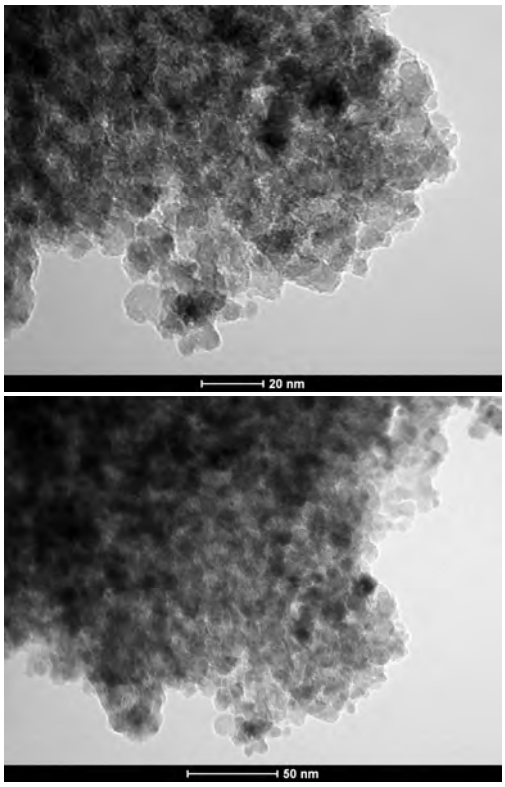

Fig. 4. TEM microphotographs of 10.9% SnO_2 powder
Rys. 4. Mikrofotografie TEM proszku 10,9% SnO_2

The obtained nanopowders are characterized by a significantly expanded specific surface area (Table 2). The mean particle sizes estimated on this basis are similar to the crystallites sizes specified by XRD, which also suggests low particle agglomeration, and undoubtedly shall have a beneficial effect on the interaction mechanism between the obtained nanopowders and the gas phase. Poorly agglomerated powders with a greatly expanded specific surface area have more active sites where the adsorption of gas substrates takes place, which gives them better selectivity and higher sensitivity to gas presence in comparison to more agglomerated powders.

Optical properties

The spectral dependence of the diffuse reflection coefficient R_{diff} (λ) of the obtained materials is presented in Figure 5.

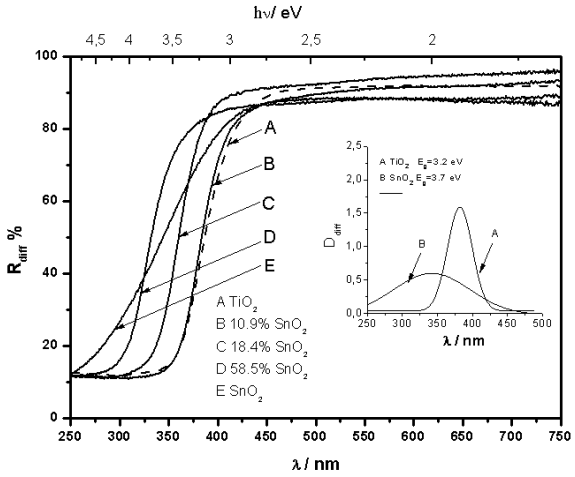

Fig. 5. Spectral dependence of diffuse reflection coefficient R_{diff} (λ) of obtained materials
Rys. 5. Spektralna zależność współczynnika odbicia dyfuzyjnego R_{diff} (λ) uzyskanych materiałów

For the purpose of comparison, the figure also contains data for SnO_2. The spectral reflectance for a semiconductor in the form of a powder (Fig. 5) is characterized by a narrow spectral region in which rapid linear growth of the diffuse reflection coefficient (R_{diff}) occurs. The band gap energy (E_g) values for titanium oxide and tin oxide were estimated based on differential spectrums as extreme: $D_{diff} = dR_{diff}/d\lambda$. The intraband absorption limit for TiO_2 and the nanocomposite containing 10.9% SnO_2 occurs at a wavelength of approx. 380 nm. As the amount of tin(IV) oxide rises, the limit shifts towards higher energy. As for SnO_2, a change in the $R_{diff}(\lambda)$ correlation slope within the scope of strong light absorption is observed. Direct allowed transitions are present in the case of SnO_2, whereas inverted indirect transitions occur for TiO_2. The E_g values for TiO_2 (anatase) and SnO_2 (cassiterite) are estimated as 3.2 and 3.7 eV, respectively, which is consistent with the data in the literature.

CONCLUSIONS

The presented method for synthesizing nanopowders allows one to obtain composites of a known and controllable chemical composition from the TiO_2-SnO_2 system. XRD analysis proved that nanocomposites crystallize in tetragonal structures TiO_2 - anatase and SnO_2 - cassiterite. The obtained nanopowders are characterized by significant expansion of the specific surface area (SSA~100 m^2/g) and the crystallite size specified by means of XRD was estimated at approx. 8 nm. An addition of SnO_2 to pure TiO_2 results in the interband absorption limit in the semiconductor shifting towards higher energy. Modification of the nanocomposites electron configuration has a beneficial effect on the electric charge transport at the grain boundary of both oxides.

Acknowledgments

This paper was financially supported by the Polish Ministry of Science and Higher Education under AGH University project no. 11.11.160.617.

REFERENCES

[1] Moon W.J., Yu J.H., Choi G.M., Selective gas detection of SnO_2-TiO_2 gas sensors, J. Electron. 2004, 13, 707-713.

[2] Radecka M., Kusior A., Lacz A., Trenczek-Zajac A., Lyson--Sypien B., Zakrzewska K., Nanocrystalline TiO_2/SnO_2 composites for gas sensors, J. Therm. Anal. Calorim. 2012, 108, 1079-1084.

[3] Carotta M.C., Gherardi S., Guidi V., Malagu C., Martinelli G., Vendemiati B., Sacerdoti M., Ghiotti G., Morandi S., Bismuto A., Maddalena P., Setaro A., (Ti, Sn)O_2 binary solid solutions for gas sensing: Spectroscopic, optical and transport properties, Sens. Actuators B 2008, 130, 38-45.

[4] Zeng W., Liu T., Wang Z., Sensitivity improvement of TiO_2 - doped SnO_2 to volatile organic compounds, Physica E 2010, 43, 633-638.

[5] Kusior A., Radecka M., Zych Ł., Zakrzewska K., Reszka A., Kowalski B.J., Sensitization of TiO_2/SnO_2 nanocomposites for gas detection, Sensors and Actuators: B Chemical 2013, 189, 251-259.

[6] Radecka M., Zakrzewska K., Rękas M., SnO_2 -TiO_2 solid solutions for gas sensors, Sensors and Actuators: B Chemical 1998, 47, 193-203.

[7] Kenanakis G., Vernardou D., Koudoumasa E., Kiriakidis G., Katsarakis N., Ozone sensing properties of ZnO nanostructures grown by the aqueous chemical growth technique, Sensors and Actuators B 2007, 124, 187-190.

[8] Shimizu Y., Jono A., Hyodo T., Egashira M., Preparation of large mesoporous SnO_2 powder for gas sensor application, Sensors and Actuators B 2005, 108, 56-61.

[9] Renganathan B., Sastikumar D., Gobi G., Rajeswari Yogamalar N., Chandra Bose A., Nanocrystalline ZnO coated fiber optic sensor for ammonia gas detection, Optics and Laser Technology 2011, 43, 1398-1404.

